

Correlation of pH-dependent surface interaction forces to amino acid adsorption: Implications for the origin of life

HUGH CHURCHILL,¹ HENRY TENG,² AND ROBERT M. HAZEN^{3,*}

¹Department of Physics, Oberlin College, Oberlin, Ohio 44074, U.S.A.

²Department of Earth and Environmental Sciences, George Washington University, Washington, D.C. 20006, U.S.A.

³Carnegie Institution of Washington and NASA Astrobiology Institute, Washington, D.C. 20015, U.S.A.

ABSTRACT

We used an atomic force microscope (AFM) with a modified tip to measure interaction forces between a silica microsphere and surfaces of quartz, calcite, and albite over a range of pH. Minima in the magnitude of electrostatic repulsion or attraction appeared near the point of zero charge (pH_{pzc}) values for quartz (≈ 2.8), calcite (9.5), albite (2.6), and silica glass (3.5). We observed small, but significant, differences in pH_{pzc} values for the (100), (101), and (011) faces of quartz. In order to correlate mineral surface charges with ionic characteristics and corresponding isoelectric points (pI) of amino acids, we immersed quartz and calcite in solutions of six amino acids. Quartz ($\text{pH}_{\text{pzc}} \approx 2.8$) tends to adsorb amino acids most strongly when pH_{pzc} and pI differ significantly. Thus quartz adsorbs lysine (pI = 9.74) more strongly than amino acids with lower pI. In contrast, calcite ($\text{pH}_{\text{pzc}} = 9.5$) adsorbs a variety of amino acids with a range of pI. Calcite thus represents a more plausible template than quartz for prebiotic selection and organization of homochiral polypeptides.

INTRODUCTION

Chiral mineral surfaces have the ability to adsorb selectively left- vs. right-handed molecules (Lahav 1999; Hazen and Sholl 2003). Face-specific, stereoselective adsorption of amino acids onto mineral surfaces has thus been proposed as a viable mechanism to account for the origins of biological homochirality, as manifest in the exclusive incorporation of left-handed amino acids and right-handed sugars in biological organisms (Lahav 1999; Hazen et al. 2001). Enantiomeric selection on crystalline surfaces, furthermore, presents a promising avenue for chiral purification of pharmaceuticals and in other industrial applications (Jacoby 2002). In order to evaluate this surface selection process, however, we must first understand adsorption mechanisms and environmental factors that influence those mechanisms.

Of fundamental importance to these studies are measurements of interactions that occur on *specific* crystal faces, as opposed to bulk measurements from polycrystalline samples. Many aspects of mineral surfaces, including atomic structure (Hazen 2004; Downs and Hazen 2004), topographic features such as etch pits (Joshi et al. 1970; Joshi and Paul 1977; Teng et al. 1998), and electrochemical properties such as surface potential (Parsons 1990), vary for different crystallographic faces of a given crystal. Of special interest is stereoselective adsorption that occurs on mirror-related crystal faces (McFadden et al. 1996; Sholl 1998; Hazen et al. 2001; Kahr and Gurney 2001). Characterizations of these properties must be conducted on specific crystal faces if they are to be relevant to understanding stereoselective adsorption of amino acids by mineral surfaces.

Here we report two complementary sets of face-specific measurements for the common rock-forming minerals quartz, calcite, and albite. First, we determined the point of zero charge (pH_{pzc})

of specific crystal surfaces based on the interactive force between AFM (atomic force microscopy) tips and mineral surfaces. The occurrence of pH_{pzc} is fundamentally important to many processes occurring at the mineral-water interface, including adsorption (Riese 1983; Dzombak and Morel 1990; Parks 1990), dissolution and precipitation (Stumm and Wieland 1990; Stumm 1992), and colloid formation (Shchukin et al. 2001). Above the pH_{pzc} , minerals display negative surface charge, whereas below the pH_{pzc} a positive charge occurs. Although the amount of surface charge at pH conditions other than pH_{pzc} depends upon the nature of the surface reactions for different minerals, the occurrence of pH_{pzc} marks a changeover in surface electrochemical properties. The most common method for determining the pH_{pzc} of a mineral is acid-base titration of solid suspensions. However, this method relies on crushed or powdered minerals in solution and therefore yields only a weighted average of all crystal faces rather than a face-specific determination of surface charge.

In addition, we determined the relative adsorption of different amino acids (with different isoelectric points) onto quartz and calcite surfaces. Amino acids are zwitterions and therefore exhibit pH-dependent electrical properties analogous to those of mineral surfaces. The isoelectric point (pI) of an amino acid is the solution pH at which that amino acid carries equal amounts of positive and negative charges. At pH values above the pI amino acids become anionic, whereas below the pI amino acids become cationic. Thus, we probe the influence on adsorption by electrostatic/ionic interactions based on the pH_{pzc} value of a mineral and the pI values of amino acids in these selective adsorption experiments.

AFM force measurements and surface electric properties

In the past decade, the advent of force scanning microscopy has led to the development of several techniques that are potentially capable of probing crystal face-specific interactions,

* E-mail: r.hazen@gl.ciw.edu

including ionization of surface functional groups. The essence of these AFM techniques lies in the measurement of interactive forces between AFM tips and sample surfaces (e.g., Butt et al. 1995; Cappella and Dietler 1999; Lower et al. 2000, 2001), and the key difference between these techniques is whether and how the tips are pre-treated.

Three levels of sophistication can be achieved in AFM force measurement based upon the tips used. On a rudimentary level, pristine cantilevers with no add-ons or extra coatings are used to directly observe the interactive forces between a tip and a flat surface. Studies using this approach (e.g., Weisenhorn et al. 1989; Burnham et al. 1990; Eggleston and Jordan 1998) are highly successful in demonstrating the potential of AFM to probe surface electric properties and measure surface free energies. Unfortunately, comparison of force measurements with theory proved difficult because, except a few cases (e.g., Burnham et al. 1990), the geometry and sizes of pristine tips were not well defined.

A more advanced approach, colloidal probe microscopy, employs a modified AFM cantilever that has a well-defined micrometer-scale sphere attached to perform the function of a microfabricated tip (Ducker et al. 1991, 1992; Johnson et al. 1995). With its better-defined probe radius, this technique has an advantage of being able to provide force measurements that agree well with theoretical predictions (Ducker et al. 1991, 1992). Additionally, the modified cantilever seems to enhance the reproducibility of force measurements, either from the same probe at different conditions, or from different probes (Ducker et al. 1992). On the negative side, the large size of the spheres (usually a few micrometers in diameter) precludes molecular-scale force mapping and the observation of individual surface functional groups.

Direct probing of molecular processes on solid surfaces becomes achievable with the development of chemical force microscopy (CFM), which uses functionalized tips (Frisbie et al. 1994; Noy et al. 1997; Okabe et al. 2000). To perform force measurements using CFM, pristine AFM cantilevers are modified by allowing formation of a self-assembled monolayer (SAM) on the tips. Commonly used SAMs include alkyl thiols (for Au coated tips) and silanes (for Si-based tips) that contain a variety of terminal organic functional groups. These functional groups are very robust and stable because the SAMs are covalently linked to the tip surfaces.

The most significant advantage of functionalized AFM tips is that they allow direct measurement of interactive forces between distinct chemical groups on surfaces. Noy et al. (1997) estimated that for tips with a typical radius of 30 nm, there are only 15–25 molecular contacts in non-polar solvents and about 200 ions involved in electrolyte solutions for tip-surface interactions. The small numbers of contacting surface groups indicate that local forces rather than average interactions may be probed by the CFM technique.

Relevant AFM force measurements can be correlated to surface electric properties by monitoring the transition of adhesive-repulsive forces with changing pH. In the absence of surface charges, interactive forces between tips and surfaces are dominated by Van der Waals attraction or hydrogen bonding between functional groups on tips and surfaces. As a result,

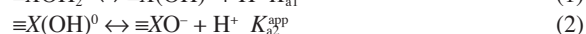
AFM force measurements are characterized by strong adhesion between tips and surfaces. For surface functional groups that undergo protonation/deprotonation to produce surface charges, the adhesive force gives rise to repulsion when tips and surfaces bear the same charge, but that force becomes zero when charges on tips or surfaces are neutral. The pH at which this transition occurs is interpreted to approximate the pH_{pzc} of a surface or the pK of the functional groups involved.

It is noteworthy to point out that, regardless of the tips used, all studies using AFM force measurements observed the pH-dependent changes of interactive forces between tips and surfaces in electrolyte solutions. For example, using CFM, Noy et al. (1997) demonstrated a quick fade of adhesion force with changing pH for COOH-COOH and COOH-OH interactions. The authors interpreted the transition pH to be the pK of the surface COOH groups. Eggleston and Jordan (1998) observed a minimal to negative repulsion on synthetic quartz and hematite near the expected pH_{pzc} using pristine tips. In the present study, we employed the approach of colloidal force microscopy to measure the interactive forces between a silica microsphere and mineral surfaces over a range of pH. To our knowledge there has been no attempt (except on mica) using chemical force microscopic method and only one successful case using pristine AFM tips for pH_{pzc} measurements of specific mineral surfaces (Eggleston and Jordan 1998). Here we show the potential of colloidal force microscopy as a tool to probe pH_{pzc} on mineral surfaces.

Development of surface charge

Development of surface charges on minerals exposed to aqueous environments can be understood as a consequence of surface complexation, by which water molecules form chemical bonds with under-coordinated surface ions via chemisorption (Schindler and Stumm 1987; Dzombak and Morel 1990). These surface-bound water molecules are then subject to a proton transfer process that shifts hydrogen ions onto neighboring surface anions. For (hydr)oxide materials, this dissociative sorption of water molecules results in a hydroxylated surface on which the reactive sites are surface hydroxyl groups $\equiv\text{X}(\text{OH})^0$ where \equiv symbolizes lattice bond and X represents cation component of the (hydr)oxide. James and Parks (1982) reported that hydroxylation of many metal oxide surfaces proceeds to completion in air at relative humidity levels $\ll 1\%$.

When brought into contact with aqueous solutions, hydroxyl groups of surface sites can undergo protonation or deprotonation to form charged surface species $\equiv\text{XOH}_2^+$ and $\equiv\text{XO}^-$, respectively. The relative abundance of protonated and deprotonated species thus governs the surface charge of the (hydr)oxide material in the absence of adsorbing ions other than H^+ . Surface ionization reactions responsible for the amphoteric (i.e., simultaneous acidic and basic) behavior of the surface hydroxyl group may be expressed by



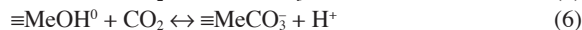
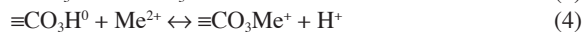
where K_{a1}^{app} and K_{a2}^{app} are apparent equilibrium constants for reactions in Equations 1 and 2, or apparent acidity constants for surface species $\equiv\text{XOH}_2^+$ and $\equiv\text{X}(\text{OH})^0$, respectively (Dzombak

and Morel 1990). K^{app} is a function of surface charge and varies with experimental conditions, but can be related to the intrinsic equilibrium constant through surface potential. Equations 1 and 2 reveal that the relative concentrations of the protonated and deprotonated surface sites, and hence the surface charge, are controlled by the pH of the aqueous environment. The pH with equal amounts of $\equiv\text{XOH}_2^+$ and $\equiv\text{XO}^-$ results in an uncharged surface, and is defined as the pH of zero net proton charge, below which the surface is positively charged because $\equiv\text{XOH}_2^+ > \equiv\text{XO}^-$ and above which the surface is negatively charged due to the excess of $\equiv\text{XO}^-$. In the presence of adsorbing ions other than H^+ competitive complexation may occur as these ions exchange for H^+ and OH^- at $\equiv\text{X}(\text{OH})^0$ sites—a process that results in the development of other anion or cation surface complexes (Dzombak and Morel 1990) or even ternary surface complexes (Schindler and Stumm 1987). Such competitive complexation requires a more general point of zero charge (pH_{pzc}) to describe the pH at which the numbers of positively and negatively charged surface species are equal.

The average pH_{pzc} of a mineral is routinely determined by acid-base titrations of powder suspensions. The majority of titration data for (hydr)oxides can be rationalized in terms of the acid-base chemistry and the complexation equilibria of a single hydroxyl surface site, $\equiv\text{X}(\text{OH})^0$. This simplification arises because the anion of oxide minerals is O and hydration leads to a surface consisting only of hydroxylated cation centers. The existence of $\equiv\text{X}(\text{OH})^0$ groups on oxides and aluminosilicates is supported by a variety of experiments. For example, infrared spectroscopic studies of quartz and feldspars have identified the appearance of terminal surface $\equiv\text{Si}(\text{OH})^0$ groups (Iler 1979; Boehm and Knozinger 1983; Bergna 1994; Koretsky et al. 1997). Although definitive evidence supporting the existence of surface aluminum hydroxyl groups on feldspar has not been obtained (Koretsky et al. 1997), the detection of such groups on alumina, particularly $\gamma\text{-Al}_2\text{O}_3$ that contains both tetrahedrally and octahedrally coordinated Al, has convinced many investigators of the presence of some type of hydroxylated aluminum surface groups, such as $\equiv\text{Al}(\text{OH})^0$, $\equiv\text{Al}(\text{OH})_2^+$, $\equiv\text{Al}(\text{OH})^-$, $\equiv\text{Al}(\text{OH})_2^+$, and $\equiv\text{Al}(\text{OH})\text{-Si}$ (Casey et al. 1989; Brady and Walther 1989; Blum and Lasaga 1991; Hellmann 1995; Koretsky et al. 1997).

While a single-site model is sufficient to account for surface complexation on oxide materials, more types of sites have to be taken into consideration when dissociative adsorption of water molecules takes place on surfaces of salt-type minerals. As in the case of oxides, a proton transfer process leads to hydroxylated surface cation centers on salt minerals. However, unlike oxides, protonation of surface anion of salts results in a different type of non-hydroxylated surface anion site $\equiv\text{AH}^0$, where A is the anion of the salt mineral. Stipp and Hochella (1991) examined calcite surfaces exposed to water using X-ray photoelectron spectroscopy and low-energy electron diffraction and found direct evidence for $\equiv\text{CO}_3\text{H}^0$ and $\equiv\text{CaOH}^0$ sites. Van Cappellen et al. (1993) modeled the carbonate mineral-aqueous solutions interface by assuming that hydration of a carbonate mineral surface produces two types of sites: $\equiv\text{Me}(\text{OH})^0$ and $\equiv\text{CO}_3\text{H}^0$, where Me is the divalent metal of the carbonate. Noting the occurrence of $\equiv\text{CO}_3\text{H}^0$ and the rapid dissolution/precipitation kinetics, they proposed the following reactions, in addition to Equations 1 and 2, to govern surface

speciation in the $\text{MeCO}_3\text{-H}_2\text{O-CO}_2$ system:



Their model matched the observed dependence of MnCO_3 surface charge on pH and pCO_2 and adequately correlated surface speciation with the experimental measured dissolution kinetics of calcite.

In our experiments we find that these significant differences in surface complexation of quartz vs. calcite play an important role in their relative adsorption of different amino acids.

EXPERIMENTAL METHODS

Force measurement

We used a Digital Instruments Nanoscope IIIa Multimode AFM with a fluid cell to immerse samples in an aqueous solution. Samples of natural quartz approximately $5 \times 5 \times 1$ mm were cut from {100}, {101}, and {011} faces of crystals obtained from a quartz mine near Hot Springs, Arkansas (Ron Coleman Mining, Inc.). Similar chips were cut from (104) cleavage surfaces of calcite from the Elmwood mine, Carthage, Tennessee, and from (001) cleavage surfaces of albite from Amelia Courthouse, Virginia (National Museum of Natural History specimen number C5390).

Mineral samples were cleaned successively with distilled deionized water, chloroform, hexane, chloroform, and distilled deionized water. However, AFM surface images of the quartz samples obtained after this cleaning revealed a thin residual organic surface film. Subsequent cleaning in an ultrasonic bath for 1 min, first in 10% HCl and then in chloroform, removed this film. All samples except calcite were stored in distilled deionized water to minimize further contamination.

Measurements of quartz surface interaction forces were conducted in solutions with pH values ranging from 2 to 11. For calcite, measurements were taken from pH 9 to 11, and albite measurements were conducted in the pH range 2 to 3.2. All pH measurements were made using an Oakton pH 2500 meter combined with a Cole Palmer general-purpose electrode and a stainless steel automatic temperature-compensation probe, which has an estimated precision of ± 0.01 . The pH series solutions for the quartz and albite experiments were created from two stock 0.01 M solutions of NaCl. One stock solution was adjusted down in pH using 1.0 N HCl, and the other was adjusted up in pH using 1.0 N NaOH. After allowing the solution to equilibrate for 15 minutes at each desired pH, we removed 2 mL from the stock solution and placed it in a vial for later application onto the mineral surfaces. Because of the high solubility of calcite in water, we employed near-equilibrium solutions with respect to calcite instead of distilled deionized water to produce the pH series for the calcite experiments. A stock solution in equilibrium with calcite was prepared to have concentrations of 2.46×10^{-5} M $\text{CaCl}_2 \cdot 2\text{H}_2\text{O}$ (Aldrich 99.99%) and 1.00×10^{-5} M NaHCO_3 (Aldrich 99.99%) and an ionic strength of 3.21×10^{-5} molal. The saturation state and the ionic strength of the stock solution were determined using the numerical code MINTQA2 (Allison et al. 1991); we assumed an open system and $\text{pCO}_2 = 10^{-3.5}$ atmosphere. The solution was then adjusted in pH with 1.0 N NaOH to prepare the pH series for the calcite experiments.

Prepared mineral samples were first imaged using contact mode AFM to ensure that the force measurements were conducted on flat surface areas. AFM images of these flat areas are often featureless. Force measurements were conducted without the O-ring attached to the fluid cell, and 25 μL of solution was pipetted directly onto the mineral surfaces before each measurement. Experiments started either at the high end of the pH range and worked down or started at the low end and worked up. Following each measurement, we removed all residual solution from both the mineral surface and the AFM probe using Kimwipes, then pipetted distilled deionized water onto the surface to rinse off the old solution. The surface was dried again using Kimwipes before the next measurement.

Standard silicon nitride AFM cantilevers were modified using the colloid probe technique introduced by Ducker et al. (1991). The procedure for applying 6.8 μm diameter silica microspheres to the cantilevers employed a dilute suspension of microspheres, which was transferred onto a freshly cleaved mica surface mounted on the AFM sample puck. We heated the puck to evaporate the fluid portion of

the suspension. Once the puck had been attached to the AFM, we placed a drop of epoxy on the mica to the left of the cantilever deflection laser. We positioned the end of the cantilever above the edge of the epoxy and lowered it to collect a small amount of epoxy on the bottom of the cantilever. Then we moved the cantilever over a silica microsphere, which was glued to the end of the cantilever (Fig. 1). Prior to tip modification the microspheres were cleaned ultrasonically to remove any coatings associated with the manufacturing process.

Data collected from the AFM was in the form of cantilever deflection vs. cantilever z -position. These force curves, which we produced by lowering the modified cantilever onto the crystal surface, typically reveal three distinctive kinds of surface interactions (Fig. 2). Prior to lowering the tip the cantilever deflection is zero. The first interaction between the tip and the crystal surface is usually a slight initial repulsion or attraction, which bends the tip away from or toward the surface and thus causes a cantilever deflection. The magnitude of this deflection is directly related to the surface charge of the crystal. As the tip is lowered further, this initial deflection is typically followed by an abrupt onset of Van der Waals attraction that leads to a “snap down” of the tip and a strong negative deflection. Once in contact with the crystal surface, further lowering of the cantilever leads to an increased force and positive deflection as the tip is bent back (constant compliance). Because it is difficult to separate Van der Waals effects from electrostatic interactions on retraction curves, only measurements collected on probe-sample approach curves were used.

In cases where electrostatic interactions are the sole forces (i.e., short-ranged

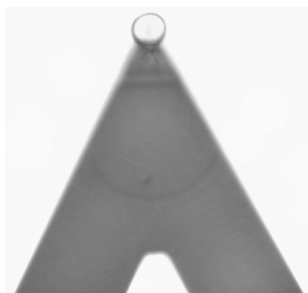


FIGURE 1. A modified standard Si_3N_4 AFM cantilever with a $6.8 \mu\text{m}$ silica microsphere attached to the tip.

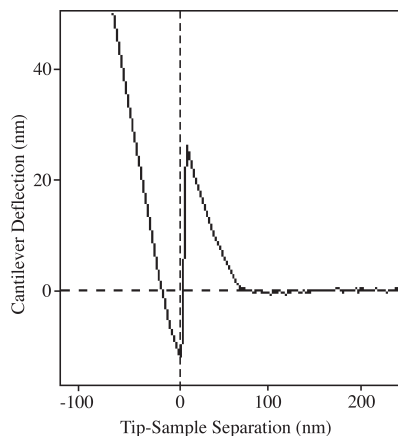


FIGURE 2. A typical force curve displays cantilever height (z in nm) above a quartz (100) surface vs. the cantilever deflection. This force curve (for pH = 11) reveals three kinds of surface interactions. (a) As the tip approaches the surface an initial electrostatic repulsion bends the tip away from the surface and thus causes a positive cantilever deflection. The magnitude of this deflection is related to the crystal’s surface charge. (b) As the tip is lowered further, this initial positive deflection is typically followed by an abrupt onset of Van der Waals attraction that leads to a “snap down” of the tip and a negative deflection. (c) Once in contact with the crystal surface, further lowering of the cantilever leads to an increased force and positive deflection as the tip is bent back.

Van der Waals forces are negligible) and surface potential is small ($< \sim 50$ mV), comparison of cantilever deflections over a range of pH provides a relative measure of the mineral surface charge through application of the following relations:

$$k_c \Delta z_c = F_{el} = \frac{4\pi R \sigma_1 \sigma_2}{\epsilon \epsilon_0 k} \times e^{-\kappa D} \quad (7)$$

where k_c is the spring constant of the cantilever, Δz_c is the cantilever deflection, F_{el} is the electrostatic force of interaction between a spherical tip and a flat sample, R is the radius of the sphere, σ_1 and σ_2 are the surface charge densities of the two surfaces, ϵ_0 is the permittivity of free space, ϵ is the dielectric constant of the medium, D is the distance between tip and sample, and κ is the inverse of the Debye length as determined by the salt concentration of the solution (Ducker et al. 1991; Carnie et al. 1994; Butt et al. 1995). Notice that Equation 7 does not describe the overall shape of the force curves because the real measurements are a convolution of Van der Waals and electrostatic interactions.

From Equation 7 it follows that a relative measure of the product of the surface charge densities of the sample and the tip may be obtained by comparing cantilever deflections over a range of pH. We did not intend to measure absolute sizes of the interactive forces due to the uncertainties in k_c and R (only approximate values are provided for the parameters by the manufacturers). Rather, by using the same probe and same surface region for all measurements on each mineral, our experiments aimed at identifying pH ranges where the tip deflection reaches a minimum on each surface. From Equation 7 it can also be seen that, because our modified cantilever has $R \sim 3.5 \mu\text{m}$ (more than two orders of magnitude greater than that of the standard AFM diamond tip), the signal-to-noise ratios of surface force measurements increase by a corresponding factor. This procedure, furthermore, averages out effects of etch pits, steps, and other nm-scale local surface features that might affect surface interaction force measurements.

We first conducted force measurements on a quartz {100} face over a wide pH range (pH 2–11) to test the sensitivity of the modified tip. Sequential measurements were then focused in the vicinity of the expected pH_{pzc} for quartz (pH 2–4 on {101} and {011} faces), feldspar (pH 2–3.2) and calcite (pH 9–11). Force curves (each averaged 3 times) were collected for each combination of mineral surface and solution pH ten to twenty times. The same surface region of the crystal was probed at different pH to ensure consistency of the measurements. Raw force data were converted into cantilever deflection vs. tip-sample separation curves using *Mathematica* with the zero for cantilever deflection defined to be the deflection at maximum tip-sample separation and the zero for tip-sample separation defined to be the z -position of the beginning of the region of constant compliance between the tip and sample. With these repetitive procedures, we were always able to obtain force curves for which the snap-down and constant compliance regions were sufficiently well defined to determine the z -zero (see Fig. 2). Cantilever deflections were measured at a distance of 10 nm above the sample surface. When the snap-down region extended more than 10 nm, the deflections before the onset of snap-down were normalized to a distance of 10 nm using Equation 7. For measurements on quartz conducted at pH 2–11, the results were normalized to ionic strength of 0.01 molal. Final results were presented as plots (Figs. 3A–D) of deflection vs. pH instead of force vs. pH because the absolute force values could not be determined without a clear knowledge of the cantilever spring constants.

Selective adsorption of amino acids

We selected three quartz crystals, each of which was approximately 6 cm in diameter with well-developed rhombohedral terminal {101} and {011} faces and prismatic {100} faces, as well as {111} faces, which are useful for distinguishing left- and right-handed crystals (Hazen 2004). We cleaned each crystal successively with deionized distilled water, chloroform, hexane, chloroform, and deionized distilled water, followed by heating for 8 h at 500 °C in a muffle furnace to remove any residual organic material. Following the cleaning process, we immersed each crystal in a beaker that contained a solution with a 2.5×10^{-3} M concentration of each of the six amino acids, alanine, aspartic acid, glutamic acid, glycine, lysine, and tyrosine, at pHs of 5, 7, and 9. After 24 h, we removed each crystal and washed it with deionized water at the pH of the immersion solution to remove any residual amino acid solution. Amino acids were desorbed from the individual crystal faces by holding the face horizontally, pipetting a pH 1 solution of HCl onto the face for 20 seconds, and then collecting the acid wash in the same pipet.

Similar procedures were employed to measure relative adsorption of different amino acids on the {104} cleavage surfaces of calcite. We powdered samples of five different natural calcite crystals—a procedure that produces microscopic {104} cleavage rhombs $< 100 \mu\text{m}$ in diameter. In the case of calcite we studied

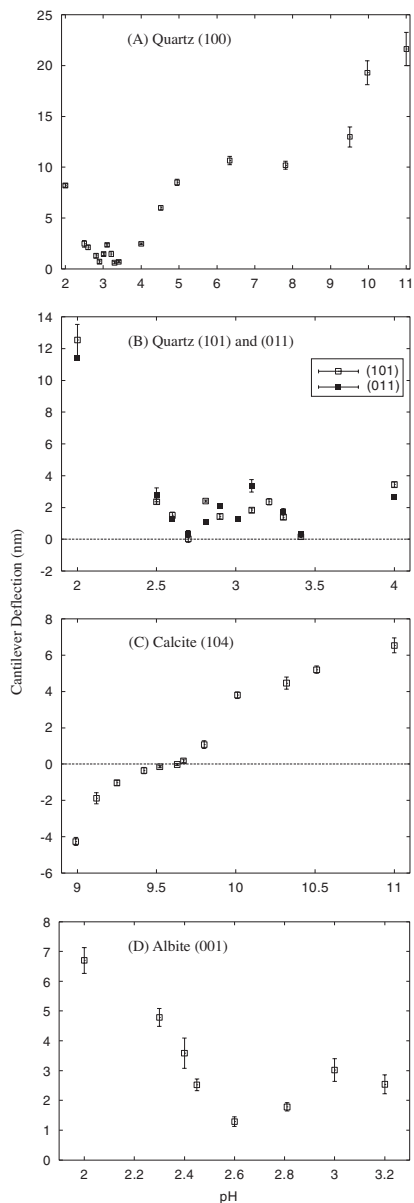


FIGURE 3. Average cantilever deflection vs. pH for mineral surfaces. **(A)** Quartz {100} surface over the pH range from 2 to 11. The pH_{pzc} of quartz is seen as a minimum at 2.9, whereas the pH_{pzc} of silica glass (the microsphere) is the minimum at 3.5. Electrostatic repulsion increases above and below these points of zero charge, corresponding to increases in the surface charge densities of the two surfaces. All results were normalized to an ionic strength of 0.01 molal. **(B)** Quartz {101} and {011} surfaces over the pH range from 2 to 4. These quartz faces have $\text{pH}_{\text{pzc}} = 2.7$, which represents a small but significant difference from the $\text{pH}_{\text{pzc}} = 2.9$ of the quartz {100} face. **(C)** Calcite {104} surface over the pH range from 9 to 11. The pH_{pzc} of calcite is observed to be at $\text{pH} = 9.5$. **(D)** Albite {001} surface over the pH range from 2.0 to 3.2. The pH_{pzc} of albite is observed to be at $\text{pH} = 2.6$.

the relative adsorption of alanine, aspartic acid, glutamic acid, glycine, leucine, and tyrosine at $\text{pH} = 8$.

Relative concentrations of adsorbed amino acids on quartz and calcite were analyzed initially by J. Brandes (University of Texas, Marine Science Institute, Port Aransas, Texas) with high-performance liquid chromatography. Additional

analyses of amino acids adsorbed on quartz were contributed by S. DeVogel (University of Colorado, INSTARR, Boulder, Colorado) with reverse phase liquid chromatography.

RESULTS AND DISCUSSION

Surface charge measurement

Quartz. Initial measurements were performed on a {100} prismatic face, as illustrated in Figure 3a. A minimum deflection occurs at $\text{pH} = 2.9 \pm 0.05$, which matches the pH_{pzc} of powdered quartz as determined by previous methods (Parks 1965; Davis and Kent 1990). We argue this minimum in surface interaction force results from the absence of surface charge on quartz, which should correspond to a minimum in the observed cantilever deflection. We did not observe a measurement of exactly zero, perhaps because the pH_{pzc} for quartz is slightly higher or lower. A second observed minimum at $\text{pH} = 3.5$ corresponds to the pH_{pzc} of the amorphous silica sphere attached to the AFM probe (Bolt 1957).

The shape of the deflection curve below $\text{pH} = 2.9$ and above $\text{pH} = 3.5$ is as expected in light of the differences between the surface (quartz) and the probe (amorphous SiO_2). Both probe and surface have an increasing positive charge below $\text{pH} = 2.9$, which exerts a repulsive force and is manifest in the observed increasing cantilever deflection. Eggleston and Jordon (1998) have suggested that significant negative surface charge does not develop on quartz surfaces until pH exceeds approximately 8 due to its widely spaced pKs. It follows from this proposal that there should be a limited repulsion between surface and probe above $\text{pH} = 3.5$. However, it has also been shown that amorphous silica develops large surface potential when pH conditions deviate from its pH_{pzc} (Higgins et al. 2002). This result implies that the repulsion can be significant and the observed cantilever deflection above $\text{pH} = 3.5$ may thus be related more to surface charge of the silica probe rather than to the quartz surface. Additionally, increasing tip deflection observed above $\text{pH} \sim 9$ may indicate a more rapid development of negative surface charge on the quartz surface, as suggested by Eggleston and Jordon (1998). Between the pH_{pzc} values of the two surfaces ($\text{pH} 2.9$ – 3.5), we expected an attractive force (negative deflection), but observed a small repulsive force in this pH range. We have no obvious explanation for this effect, but it could be due to the effects of micrometer-scale topographical features such as etch pits that are observed to have different electrostatic properties compared to the surrounding planar surfaces. This effect underscores the need for relatively pristine surfaces when conducting such measurements.

Additional surface interaction force measurements were made on {101} and {011} rhombohedral faces of quartz at pH values from 2 to 4 (Fig. 3b). Both of these faces display $\text{pH}_{\text{pzc}} = 2.7 \pm 0.05$. The difference between these values and $\text{pH}_{\text{pzc}} = 2.9$ of the {100} prismatic face is small, but significant, and it points to the importance of making such measurements on specific crystal surfaces rather than on powdered samples.

Calcite. Figure 3c displays the variation with pH of AFM cantilever deflection above a calcite crystal surface. The data, which are to our knowledge the first direct measurements of calcite surface interaction forces, suggest that $\text{pH}_{\text{pzc}} = 9.5 \pm 0.1$, in general agreement with previous estimates (Parks 1984). Due

to the relatively large difference in pH_{pzc} between calcite and amorphous silica, and the large negative surface charge buildup on silica microsphere attached to the AFM probe at $\text{pH} > 7$, strongly attractive forces were observed in the pH range between the pH_{pzc} s of the two surfaces. In pH ranges where we saw attractive forces for calcite, we observed a clear transition from zero deflection to negative deflection (attraction) before the abrupt snap-down (Fig. 4). This effect allowed us to distinguish the electrostatic attraction between the surface and the probe from Van der Waals snap-down and suggested that the crossover pH for tip deflection from repulsive to attractive is a rather accurate measure of the calcite pH_{pzc} . The relatively high sensitivity of cantilever deflection in these measurements points to the utility of wide separation in pH_{pzc} between sample and probe in studying surface electrostatic forces.

Albite. Figure 3d reveals that albite $\text{pH}_{\text{pzc}} = 2.6 \pm 0.1$. As in the quartz data, no measurement of zero deflection was found, nor did we observe a negative deflection between the pH_{pzc} of albite and that of amorphous silica. Unlike quartz, additional factors associated with preferential release of Na and Al at low pH conditions may affect the force measurements. We did not characterize the surface compositional change on albite during force measurement and therefore cannot quantify the effect of surface leaching.

Amino acid adsorption

The surface charge of a mineral should play a significant role in the adsorption of molecular species. We anticipated, for example, that amino acids with pIs differing greatly in pH from the pH_{pzc} of a mineral surface should be adsorbed in greater abundance onto the mineral surface than amino acids for which pI and pH_{pzc} are similar. This expectation draws on the fact that at pH values above the pH_{pzc} of quartz, but below the pI

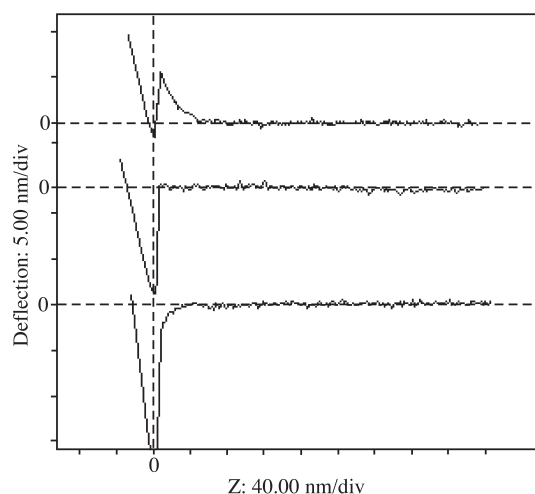


FIGURE 4. Three force curves collected on a calcite {104} surface showing repulsive (upper), near zero (middle), and attractive (lower) forces before “snap-down.” The repulsive curve was taken at pH 10.5, above the pH_{pzc} of calcite, the near zero curve was taken at pH 9.6, near the pH_{pzc} of calcite, and the attractive curve was taken at pH 9.0, below the pH_{pzc} of calcite. Repulsion and attraction are indicated by the positive and negative deflections shown in the upper and lower curves before “snap-down.”

of the amino acid, the quartz surface and the amino acid will have opposite charge so that an electrostatic attraction should occur. The greater the separation in pH between the pH_{pzc} of the mineral and the pI of the amino acid, the greater will be the charge difference between the mineral surface and the amino acid. This effect should enhance adsorption for systems in which adsorption is dominated by electrostatic interactions. To test this hypothesis, we immersed quartz and calcite in equimolar solutions of multiple amino acids to see if differential adsorption of amino acids occurs.

Previous researchers have observed selective adsorption of some amino acids onto mineral surfaces—a result that points to the broader implications of the results discussed here. Carter (1978), who compared the amino acid composition of fulvic acid adsorbed from solution onto quartz and calcite sand, documented the preference of arginine for quartz and aspartic acid for calcite. Arginine (pI = 10.76) has the highest pI of all biological amino acids, while aspartic acid (pI = 2.98) has the lowest pI. By contrast, the pH_{pzc} of quartz is relatively low (~2.8), whereas our observed value for calcite is relatively high (9.5). These data strengthen the idea that minerals will preferentially adsorb amino acids that have pI values significantly separated in pH from the pH_{pzc} of the mineral.

Quartz. Based on the surface charge properties of quartz, we anticipated that an amino acid such as lysine with a relatively high isoelectric point should adsorb more efficiently onto quartz than amino acids with lower pI values. Indeed, in experiments with equimolar concentrations of alanine (pI = 6.11), aspartic acid (pI = 2.98), glutamic acid (pI = 3.08), glycine (6.06), lysine (pI = 9.74), and tyrosine (pI = 5.63), lysine was consistently adsorbed to a greater extent than the other amino acids in the solution (Table 1). We conducted 26 experiments on separate crystal faces at three different pHs (5, 7, and 9), of which nine experiments yielded adsorbed amino acids in amounts measurable by high-performance liquid chromatography. In eight of these analyses lysine was the only amino acid detected in significant quantities, while one analysis also showed a small amount of adsorbed tyrosine (though less than 20% of the lysine concentration in that experiment).

These samples were reanalyzed with reverse phase liquid chromatography, which is particularly sensitive to the relative amounts of aspartic acid, glutamic acid, glycine, alanine, and tyrosine. We found adsorption concentrations in the following sequence: tyrosine > alanine > glycine > glutamic acid ~ aspartic acid (Table 1). Thus, glutamic acid and aspartic acid, which have pI similar to the pH_{pzc} of quartz, are the least adsorbed

TABLE 1. Relative adsorption of amino acids on quartz and calcite

*Quartz, analyzed by high-performance liquid chromatography					
Asp	Glu	Gly	Ala	Tyr	Lys
<0.05	<0.05	<0.05	<0.05	<0.20	1.00
†Quartz, analyzed by reverse-phase liquid chromatography					
Asp	Glu	Gly	Ala	Tyr	Lys
0.12	0.12	0.51	0.81	1.00	§
‡Calcite, analyzed by high-performance liquid chromatography					
Asp	Glu	Gly	Ala	Tyr	Leu
0.96	1.00	0.97	0.98	0.81	0.83

* Measurements were normalized with respect to that of Lys.

† Measurements were normalized with respect to that of Tyr.

‡ Measurements were normalized with respect to that of Glu.

§ Not detected by this analytical procedure.

amino acids.

This result supports the hypothesis that electrostatic/ionic interactions play a significant role in the adsorption of some molecular species. In this regard, some mineral surfaces have the ability to select and concentrate specific molecules from a complex suite of species – a trait that may have influenced prebiotic processes. Note, however, that this result casts doubt on the prebiotic role of quartz in establishing biological homochirality. Quartz does not efficiently adsorb such key biological amino acids as alanine, glycine, aspartic acid, and glutamic acid, which are essential components of primitive biologically active polypeptides.

Calcite. Our results for the adsorption of multiple amino acids on {104} cleavage surfaces of calcite contrast with those for quartz (Table 1). As noted by previous authors (Carter 1978; Lowenstam and Weiner 1989; Weiner and Addadi 1997), calcite displays an affinity for aspartic and glutamic acids—both amino acids with relatively low pI compared to calcite's high pH_{pzc} . However, our adsorption results (Table 1) reveal that calcite adsorbs all six of the amino acids studied to a significant degree.

This result underscores important differences in the surface atomic structure of quartz vs. calcite (Hazen 2004). Models of the quartz surface suggest a relatively uniform distribution of terminal O atoms, which achieve a neutral surface charge through hydration. Calcite, by contrast, has both O and calcium atoms at {104} surfaces. Such calcite surfaces likely possess an array of both positive and negative charge centers at any pH. Thus calcite surfaces can bond with the positive (NH_3^+) and negative ($COOH^-$) groups of any amino acid. Calcite is consequently less selective than quartz in its adsorption of amino acids.

This characteristic of calcite points to its possible role in the prebiotic selection and assembly of chiral amino acids into macromolecules of biological interest. Calcite crystals commonly develop chiral {214} scalenohedral faces, which selectively adsorb D- and L-amino acids (Hazen et al. 2001). These faces feature significant surface topography at the atomic scale, with prominent 2 Å deep linear grooves that might serve to align arrays of homochiral amino acids (Hazen 2004). These calcite surfaces thus represent a plausible symmetry-breaking environment for life's distinctive molecular handedness.

We conclude that the average charges of mineral surfaces and amino acids play a clear role in molecular adsorption, but other important factors also come into play. In particular, the geometrical distribution of positive and negative charge centers associated with specific mineral surfaces and individual amino acids dominate the adsorption process.

ACKNOWLEDGMENTS

We gratefully acknowledge T. Gooding (Smithsonian Institution, National Museum of Natural History) for assistance in sample preparation. J. Brandes (University of Texas Marine Science Institute) and S. DeVogel (University of Colorado, INSTARR) provided amino acid analyses. S. Lower (University of Maryland) provided advice on the colloid probe technique. We are grateful for valuable comments, suggestions and corrections from A. Asthagiri, C. Eggleston, M. Ewell, K. Rosso, B. Watson, and an anonymous reviewer. This work was supported by NSF (EAR0229634), the NASA Astrobiology Institute, and the Carnegie Institution of Washington.

REFERENCES CITED

Allison, J.D., Brown, D.S., and Nove-Gradac, K.J. (1991) MINTEQA2/PRODEFA2, A geochemical assessment model for environmental systems:

- Version 3.0 User's Manual. U.S. Environmental Protection Agency, Athens, Georgia.
- Bergna, H.E. (1994) Colloid chemistry of silica: An Overview. In H.E. Bergna, Ed., The colloid chemistry of silica, p. 1–47. American Chemical Society, Washington, D.C.
- Blum, A.E. and Lasaga, A.C. (1991) The role of surface speciation in the dissolution of albite. *Geochimica et Cosmochimica Acta*, 55, 2193–2201.
- Boehm, H. and Knozinger, H. (1983) Nature and estimation of functional groups on solid surfaces. In J.R. Anderson and M. Boudart, Eds., *Catalysis science and technology*, 4, 39–207. Springer-Verlag, New York.
- Bolt, G.H. (1957) Determination of the charge density of silica sols. *Journal of Physical Chemistry*, 61, 1166–1169.
- Brady, P.V. and Walther, J.V. (1989) Controls on silicate dissolution rates in neutral and basic pH solution at 25 °C. *Geochimica et Cosmochimica Acta*, 53, 2823–2830.
- Burnham, N.A., Dominquez, D.D., Mowery, R.L., and Colton, R.J. (1990) Probing the surface forces of monolayer films with an atomic-force microscope. *Physical Review Letters*, 64, 1931–1934.
- Butt, H.-J., Jaschke, M., and Ducker, W. (1995) Measuring surface forces in aqueous solution with the atomic force microscope. *Bioelectrochemistry and Bioenergetics*, 38, 191–201.
- Cappella, B. and Dietler, G. (1999) Distance curves by atomic force microscopy. *Surface Science Reports*, 34, 1–104.
- Carnie, S.L., Chan, D.Y.C., and Gunnig, J.S. (1994) Electrical double-layer interaction between dissimilar spherical colloidal particles and between a sphere and a plate: The linearized Poisson-Boltzmann theory. *Langmuir*, 10, 2993–3009.
- Carter, P.W. (1978) Adsorption of amino acid-containing organic matter by calcite and quartz. *Geochimica et Cosmochimica Acta*, 42, 1239–1242.
- Casey, W.H., Westrich, H.R., Arnold, G.W., and Banfield, J.F. (1989) The surface chemistry of dissolving labradorite feldspar. *Geochimica et Cosmochimica Acta*, 53, 821–832.
- Davis, J.A. and Kent, D.B. (1990) Surface complexation modeling in aqueous geochemistry. In M.F. Hochella Jr. and A.F. White, Eds., *Mineral-water interface geochemistry*, 23, p. 177–259. Reviews in Mineralogy, Mineralogical Society of America, Washington, D.C.
- Downs, R.T. and Hazen, R.M. (2004) Chiral indices of crystalline surfaces as a measure of enantioselective potential. *Journal of Molecular Catalysis*, in press.
- Ducker, W.A., Senden, T.J., and Pashley, R.M. (1991) Direct measurements of colloidal forces using an atomic force microscope. *Nature*, 353, 239–241.
- — — (1992) Measurements of forces in liquids using a force microscope. *Langmuir*, 8, 1831–1836.
- Dzombak, D.A. and Morel, F.M.M. (1990) *Surface Complexation Modeling*. Wiley, New York.
- Eggleston, C. and Jordan, G. (1998) A new approach to pH of point of zero charge measurement: Crystal-face specificity by scanning force microscopy (SFM). *Geochimica et Cosmochimica Acta*, 62, 1919–1923.
- Frisbie, C.D., Rozsnyai, L.F., Noy, A., Wrighton, M.S., and Lieber, C.M. (1994) Functional group imaging by chemical force microscopy. *Science*, 265, 2071–2074.
- Hazen, R.M. (2004) Chiral crystal faces of common rock-forming minerals. In G. Palyi, C. Zucchi, and L. Caglioti, Eds., *Progress in biological homochirality*. Elsevier, New York, in press.
- Hazen, R.M. and Sholl, D.S. (2003) Chiral selection on inorganic crystalline surfaces. *Nature Materials*, 2, 367–374.
- Hazen, R., Filley, T., and Goodfriend, G. (2001) Selective adsorption of L- and D-amino acids on calcite: implications for biochemical homochirality. *Proceedings of the National Academy of Sciences USA*, 98, 5487–5490.
- Hellmann, R. (1995) The albite-water system: Part II. The time evolution of the stoichiometry of dissolution as a function of pH at 100, 200, and 300 °C. *Geochimica et Cosmochimica Acta*, 59, 1669–1697.
- Higgins, S.R., Stack, A.G., Knauss, K.G., Eggleston, C.M., and Jordan, G. (2002) Probing molecular scale adsorption and dissolution-growth processes using nonlinear optical and scanning probe methods suitable for hydrothermal applications. In R. Hellmann and S. A. Wood, Eds., *Water-Rock Interactions, Ore Deposits, and Environmental Geochemistry: A Tribute to David A. Crerar*, Special Publication No. 7, pp. 111–128. The Geochemical Society, Washington, D.C.
- Iler, R.K. (1979) *The Chemistry of Silica: Solubility, Polymerization, Colloid and Surface Properties, and Biochemistry*. Wiley, New York.
- Jacoby, M. (2002) 2-D stereoselectivity. *Chemical and Engineering News*, March 25, 43–46.
- James, R.O. and Parks, G.A. (1982) Characterization of aqueous colloids by their electrical double-layer and intrinsic surface chemical properties. In E. Matijevic, Ed., *Surface and Colloid Sciences*, 12, 119–216. Plenum Press, New York.
- Johnson, S.B., Drummond, C.J., Scales, P.J., and Nishimura, S. (1995) Comparison of techniques for measuring the electrical double layer properties of surfaces in aqueous solution: hexadecyltrimethylammonium bromide self-assembly structures as a model system. *Langmuir*, 11, 2367–2375.

- Joshi, M.S. and Paul, B.K. (1977) Surface structures of trigonal bipyramidal faces of natural quartz crystals. *American Mineralogist*, 62, 122–126.
- Joshi, M.S., Kotru, P.N., and Ittiakhen, M.A. (1970) Studying dislocations in quartz by the hydrothermal-etching method. *Soviet Physics-Crystallography*, 15, 83–89.
- Kahr, B. and Gurney, R.W. (2001) Dyeing crystals. *Chemical Reviews*, 101, 893–951.
- Koretsky, C.M., Sverjensky, D.A., Salisbury, J.W., and D'Aria, D.M. (1997) Detection of surface hydroxyl species on quartz, γ -alumina, and feldspars using diffuse reflectance infrared spectroscopy. *Geochimica et Cosmochimica Acta*, 61, 2193–2210.
- Lahav, N. (1999) *Biogenesis: Theories of Life's Origin*, p. 258–259. Oxford University Press, New York.
- Lowenstam, H.A. and Weiner, S. (1989) *On Biomineralization*. Oxford University Press, New York.
- Lower, S.K., Tadanier, C.J., and Hochella Jr., M.F. (2000) Measuring interfacial and adhesion forces between bacteria and mineral surfaces with biological force microscopy. *Geochimica et Cosmochimica Acta*, 64, 3133–3139.
- Lower, S.K., Hochella Jr., M.F., and Beveridge, R.J. (2001) Bacterial recognition of mineral surfaces: nanoscale interactions between *Shewanella* and α -FeOOH. *Science*, 292, 1360–1363.
- McFadden, C.F., Cremer, P.S., and Gellman, A.J. (1996) Adsorption of chiral alcohols on "chiral" metal surfaces. *Langmuir*, 12, 2483–2487.
- Noy, A., Vezenov, D.V., and Lieber, C.M. (1997) Chemical force microscopy. *Annual Review of Materials Science*, 27, 381–421.
- Okabe, R., Akiba, U., and Fujihira, M. (2000) Chemical force microscopy of $-\text{CH}_3$ and $-\text{COOH}$ terminal groups in mixed self-assembled monolayers by pulsed-force-mode atomic force microscopy. *Applied Surface Science*, 157, 398–404.
- Parks, G.A. (1965) The isoelectric points of solid oxides, solid hydroxides, and aqueous hydroxo complex systems. *Chemical Reviews*, 65, 177–198.
- — — (1984) Surface and interfacial free energies of quartz. *Journal of Geophysical Research*, 89, 3997–4008.
- — — (1990) Surface energy and adsorption at mineral/water interfaces: an introduction. In M.F. Hochella Jr. and A.F. White, Eds., *Mineral-Water Interface Geochemistry*, 23, 133–175. Reviews in Mineralogy, Mineralogical Society of America, Washington, D.C.
- Parsons, R. (1990) Electrical double layer: Recent experimental and theoretical developments. *Chemical Reviews*, 90, 813–826.
- Riese, A.C. (1983) Adsorption of radium and thorium onto quartz and kaolinite: A comparison of solution/surface equilibrium models. Ph.D. Thesis. Colorado School of Mines, Golden, Colorado.
- Schindler, P.W. and Stumm, W. (1987) The surface chemistry of oxides, hydroxides, and oxide minerals. In W. Stumm, Ed., *Aquatic Surface Chemistry*, p. 83–110. Wiley, New York.
- Shchukin, E.D., Pertsov, A.V., Amelina, E.A., and Zelenev, A.S. (2001) Colloid and Surface chemistry. Elsevier, Amsterdam.
- Sholl, D.S. (1998) Adsorption of chiral hydrocarbons on chiral platinum surfaces. *Langmuir*, 14, 862–867.
- Stipp, S.L. and Hochella Jr., M. F. (1991) Structure and bonding environments at the calcite surface as observed with X-ray photoelectron spectroscopy (XPS) and low energy electron diffraction (LEED). *Geochimica et Cosmochimica Acta*, 55, 1723–1736.
- Stumm, W. (1992) *Chemistry of the Solid-Water Interface*. Wiley, New York.
- Stumm, W. and Wieland, E. (1990) Dissolution of oxide and silicate minerals: rates depend on surface speciation. In W. Stumm, Ed., *Aquatic Chemical Kinetics*, p. 367–400. Wiley, New York.
- Teng, H.H., Dove, P.M., Orme, C.A., and DeYoreo, J.J. (1998) The thermodynamics of calcite growth: A baseline for understanding biomineral formation. *Science*, 282, 724–727.
- Van Cappellen, P., Charlet, L., Stumm, W., and Wersin, P. (1993) A surface complexation model of the carbonate mineral-aqueous solution interface. *Geochimica et Cosmochimica Acta*, 57, 3505–3518.
- Weiner, S. and Addadi, L. (1997) Design strategies in mineralized biological materials. *Journal of Materials Chemistry*, 7, 689–702.
- Weisenhorn, A.L., Hansma, R.K., Albrecht, R.R., and Quate, C.F. (1989) Forces in atomic force microscopy in air and water. *Applied Physics Letters*, 54, 2651–2653.

MANUSCRIPT RECEIVED SEPTEMBER 16, 2003

MANUSCRIPT ACCEPTED JANUARY 29, 2004

MANUSCRIPT HANDLED BY KEVIN ROSSO